Radioactive decay by the emission of heavy nuclear fragments

O A P Tavares, L A M Roberto[1] and E L Medeiros[2]

Centro Brasileiro de Pesquisas Físicas - CBPF/MCT, Rua Dr. Xavier Sigaud 150, 22290-180 Rio de Janeiro-RJ, Brazil

Abstract - Radioactive decay of nuclei by the emission of heavy ions of C, N, O, F, Ne, Na, Mg, Al, Si, and P isotopes (known as exotic decay or cluster radioactivity) is reinvestigated within the framework of a semiempirical, one-parameter model based on a quantum mechanical, tunnelling mechanism through a potential barrier, where both centrifugal and overlapping effects are considered to half-life evaluations. This treatment appeared to be very adequate at fitting all measured half-life values for the cluster emission cases observed to date. Predictions for new heavy-ion decay cases susceptible of being detected are also reported.

PACS: 23.70.+j

Keywords: cluster radioactivity, half-life systematics, Geiger-Nuttall plots

[1]Fellow, Brazilian CNPq, contract No. 103237/2005-4.
Present address: COPPE/UFRJ, Nuclear Engineering Programme, 21945-970 Rio de Janeiro-RJ, Brazil.

[2]Author to whom correspondence should be addressed, emil@cbpf.br

1 Introduction

The spontaneous emission of heavy-ions (nuclear fragments heavier than alpha particles) from translead nuclei, known as cluster (or exotic) radioactivity, is a process firmly established since its first experimental identification from the detection of ^{14}C ions emitted from a source of ^{223}Ra isotope by Rose and Jones from the University of Oxford [1]. Such a novel radioactive decay mode was confirmed independently by Aleksandrov *et al.* [2], and soon after by Gales *et al.* [3] and Price *et al*. [4]. Mass and energy of carbon nuclei emitted in the decay of ^{223}Ra were measured in a detailed experiment by Kutschera *et al.* [5] where the ^{14}C nature of 29.8-MeV ions emitted from ^{223}Ra was unambiguously established. The half-life for such a process was obtained as $(2.1 \pm 0.5) \times 10^{15}$ s [5], thus confirming previous measurements from other laboratories [1–4].

The possible existence for such a rare radioactive decay process was reported early in 1975–1976 by de Carvalho *et al*. [6, 7], when it became clear from calculations based on the classical WKB method for penetration through a potential barrier the possibility of a few heavy-ion emission modes from ^{238}U with fragment mass in the range 20–70. Those calculations, very preliminary in nature, showed clearly that shell effects were strongly related to the decay rates, the processes involving magic numbers either for the emitted clusters or for the daughter product nuclei being the most probable fragment emission modes [8, 9] (see also [10]).

These unexpected results were interpreted soon after by Săndulescu and Greiner [11] as a case of very large asymmetry in the mass distribution of fissile nuclei caused by shell effects of one or both fission fragments [11, 12]. Later, more refined and extensive calculations by Săndulescu *et al*. [13] showed that conditions are most favorable for radioactive decay of ^{24}Ne and ^{28}Mg from Th isotopes, ^{32}Si and ^{34}Si from U isotopes, ^{46}Ar from Pu and Cm isotopes, and ^{48}Ca from Cf, Fm, and No isotopes. These early predictions were subsequently improved by new calculations [14–17] which showed that a number of heavy nuclei may exhibit a new type of decay, intermediate between alpha emission and spontaneous fission, which decay can be interpreted either as a highly mass-asymmetric fission or as an emission of a heavy nuclear cluster.

The advance in theoretical treatment of exotic decays has motivated several exper-

imental groups to develop new methods for heavy-ion identification and half-life measurements in investigating for rare cases of exotic radioactive decays of extremely small predicted branching ratio relative to alpha decay in the range $\sim 10^{-16}$–10^{-9}. Eleven different heavy clusters (^{14}C, ^{20}O, ^{23}F, $^{22,24-26}$Ne, ^{28,30}Mg, ^{32,34}Si) have been detected so far in the radioactive decay of translead parent nuclei. The reader is referred, for instance, to publications by Zamyatnin *et al*. [18], Gonçalves and Duarte [19], Guglielmetti *et al.* [20], Ardisson and Hussonnois [21], Poenaru [22], Tretyakova *et al.* [23], Kuklin *et al.* [24, 25], Hourani *et al.* [26], and references quoted therein, which give a detailed description of this phenomenon from both the experimental and theoretical points of view.

The question of why particular heavy-ion emission modes have been observed (or are the most likely candidates to be experimentally investigated) was discussed in details by Ronen [27] who, besides the aspects related to shell effects, has considered nuclei as composed of blocks of deuterons and tritons. Such a consideration led Ronen [27] to suggest the "golden rule" for cluster radioactivity as "the most favorable parents for cluster emissions are those that emit clusters which have the highest binding energy per cluster, and in which the daughter nuclei is preferably magic, close to the double magic ^{208}Pb".

The Effective Liquid Drop Model (ELDM) introduced by Gonçalves and Duarte [19] to describe the exotic decay of nuclei has been subsequently extended to proton radioactivity, alpha decay and cold fission as well, and extensive tables of partial half-life values calculated in a unified theoretical framework for all these nuclear processes became available [28].

A one-parameter model to evaluate and systematize the alpha-decay half-lives for all the possible alpha-emitting bismuth isotopes (ground-state to ground-state transitions of mutual angular momentum $\ell = 5$) has been recently developed to evaluate the alpha activity for the particular case of the naturally occurring ^{209}Bi isotope [29]. This study was motivated from the observation for the first time of an extremely low alpha activity in ^{209}Bi, equivalent to $\sim$12 disintegrations/h-kg [30]. The alpha-decay half-life for ^{209}Bi was then evaluated by the proposed model as $(1.0 \pm 0.3) \times 10^{19}$ years [29], in substantial agreement with the experimental result of $(1.9 \pm 0.2) \times 10^{19}$ years [30]. The detailed description of our semiempirical, one-parameter model is reported in [29], and it has shown to be successfully applicable to all isotopic sequences of alpha-emitter nuclides [29, 31, 32]. In particular, it has been applied in evaluating the partial alpha-decay half-lives of the Pt isotopes, where,

for the important case of the naturally occurring ^{190}Pt isotope (the radiogenic parent in the ^{190}Pt$\rightarrow^{186}$Os dating system), the model yields a half-life-value of $(3.7 \pm 0.3) \times 10^{11}$ years [31], thus very close to either the experimental determination of $(3.2 \pm 0.1) \times 10^{11}$ years obtained in the last direct counting experiment to measure the alpha activity of ^{190}Pt isotope [33] or the weighted average of $(3.9 \pm 0.2) \times 10^{11}$ years taken from all measured half-life-values available to date (for details see [31]). The same happens in discussing the rarest case of natural alpha activity ever observed due to ^{180}W isotope, for which case the evaluated half-life-value of 1.0×10^{18} years [34] agrees quite completely with the measured ones of $(1.1^{+0.8}_{-0.4}) \times 10^{18}$ years [35] and $(1.0^{+0.7}_{-0.3}) \times 10^{18}$ years [36].

One of the approaches to describe the cold cluster radioactivity of nuclei is a nonadiabatic treatment similar to alpha decay (alpha-decay-like model, ADLM) (the other approach is an adiabatic treatment similar to superasymmetric fission [24, 25]). In view of the excellent performance of our quantum-mechanical tunneling, ADLM, to all cases of alpha decay as mentioned in the precedent paragraph, we thought it worthwhile to extend our original model [29] also in systematizing the half-lives of all cases of cluster emission so far experimentally investigated. Additionally, it can be useful to evaluate half-life and/or to give half-life predictions for expected, new cases of exotic decays not yet experimentally observed. Eventually, the present proposal can also serve to investigate cases of cold fission processes, and, as it has happened with the ELDM [28], a unified semiempirical treatment can be achieved to all modes of strong nuclear decay (a description of proton radioactivity following these lines is in progress).

2 Routine calculation to half-life evaluation of cluster decay

The one-parameter model reported in details for the alpha decay process [29, 31, 32] is here adapted to calculate the half-life for the different cases of nuclear decay by emission of fragments heavier than alpha particles. In brief, the half-life for a given decay case is evaluated as

$$\tau = \log T_{1/2}, \quad T_{1/2} = T_0 \mathrm{e}^{G_{\mathsf{ov}} + G_{\mathsf{se}}}, \tag{1}$$

in which $T_0 = (\ln 2)/\lambda_0$, where λ_0 is the number of assaults on the potential barrier per unit of time, G_{ov} is Gamow's factor evaluated in the overlapping barrier region (figure 1), and G_{se} is the one associated with the external, separation region which extends from the contact configuration of the separating fragments up to the point where the total potential energy equals the Q-value for decay. In cases for which the disintegration occurs from the ground-state of the parent nucleus to the ground-state of the product nuclear fragments, and expressing lengths in fm, masses in u, energies in MeV, and time in second, the expressions for T_0, G_{ov}, and G_{se} read [29, 10]:

$$T_0 = 1.0 \times 10^{-22} a \left(\frac{\mu_0}{Q}\right)^{1/2}, \tag{2}$$

$$G_{\mathsf{ov}} = g H_{\mathsf{ov}}, \quad H_{\mathsf{ov}} = 0.4374703(c-a)\,(\mu_0 Q)^{1/2}\,(x+2y-1)^{1/2}, \tag{3}$$

$$G_{\mathsf{se}} = 0.62994186\, Z_{\mathsf{C}} Z_{\mathsf{D}} \left(\frac{\mu_0}{Q}\right)^{1/2} P(x,y), \tag{4}$$

where

$$P(x,y) = P_1(x,y) + P_2(x,y) - P_3(x,y) \tag{5}$$

with

$$P_1(x,y) = \frac{x^{1/2}}{2y} \times \ln \frac{[x(x+2y-1)]^{1/2} + x + y}{\frac{x}{y}\left[1 + \left(1 + \frac{x}{y^2}\right)^{1/2}\right]^{-1} + y}, \tag{6}$$

$$P_2(x,y) = \arccos\left\{\frac{1}{2}\left[1 - \frac{1 - \frac{1}{y}}{\left(1 + \frac{x}{y^2}\right)^{1/2}}\right]\right\}^{1/2}, \tag{7}$$

$$P_3(x,y) = \left[\frac{1}{2y}\left(1 + \frac{x}{2y} - \frac{1}{2y}\right)\right]^{1/2}, \tag{8}$$

in which the quantities x and y are calculated as

$$x = \frac{20.9008\,\ell(\ell+1)}{\mu_0 Q c^2}, \quad y = \frac{1}{2}\frac{Z_{\mathsf{C}} Z_{\mathsf{D}} e^2}{cQ}, \quad e^2 = 1.4399652\,\text{MeV·fm}. \tag{9}$$

The basic, physical quantities of the present approach are thus $a = R_{\mathsf{P}} - R_{\mathsf{C}}$, $c = R_{\mathsf{D}} + R_{\mathsf{C}}$, the reduced mass of the disintegrating system, μ_0, the Q-value for decay, and the mutual angular momentum, ℓ, associated with the rotation of the product nuclei around their common centre of mass. In equation (3) g is the adjustable parameter of the calculation

model, the value of which being thus determined from a set of measured half-life values (see below). The quantity a is the separation between the centres of the fragments not yet completely formed, from which point the fragments start to be defined and drive away from each other (the overlapping region) until the contact configuration at separation c is reached (R_{P}, R_{D}, and R_{C} denote the nuclear radius of the parent nucleus, daughter nucleus, and emitted cluster, respectively). The quantity $c - a = 2R_{\mathsf{C}} - (R_{\mathsf{P}} - R_{\mathsf{D}})$ represents, therefore, the extension of the overlapping region (see figure 1).

The values for both the quantities Q and μ_0 have been evaluated from the nuclear (rather than atomic) mass-values of the separating fragments, i.e.,

$$Q = m_{\mathsf{P}} - (m_{\mathsf{D}} + m_{\mathsf{C}}), \quad \mu_0^{-1} = m_{\mathsf{D}}^{-1} + m_{\mathsf{C}}^{-1}, \tag{10}$$

where the m's are given by

$$m_i = A_i + \frac{\Delta M_i}{F} - Z_i m_{\mathsf{e}} + \frac{10^{-6} k Z_i^{\beta}}{F}, \quad i = \mathsf{P}, \mathsf{D}, \mathsf{C}, \tag{11}$$

in which Z and A denote, respectively, the atomic number and mass number of the nuclear species, $F = 931.494009$ MeV/u is the mass-energy conversion factor, $m_{\mathsf{e}} = 0.548579911 \times 10^{-3}$ u is the electron rest mass, and ΔM is the most recent atomic mass-excess evaluation by Audi *et al.* [37]. The quantity kZ^{β} represents the total binding energy of the Z electrons in the atom, where the values $k = 8.7$ eV and $\beta = 2.517$ for nuclei of $Z \geq 60$, and $k = 13.6$ eV and $\beta = 2.408$ for $Z < 60$ have been found from data reported by Huang *et al.* [38]. In this way, the Q-value for decay is calculated as

$$Q = \Delta M_{\mathsf{P}} - (\Delta M_{\mathsf{D}} + \Delta M_{\mathsf{C}}) + 10^{-6} k \left[Z_{\mathsf{P}}^{\beta} - \left(Z_{\mathsf{D}}^{\beta} + Z_{\mathsf{C}}^{\beta} \right) \right], \tag{12}$$

where the last term in this expression represents the screening effect caused by the surrounding electrons around the nuclei.

The spherical nucleus approximation has been adopted to the present calculation model. The radii for the parent, R_{P}, and daughter, R_{D}, nuclei have been evaluated following the droplet model of atomic nuclei by Myers and Swiatecki [39, 40]. Accordingly, we have used the radius expressions for the average equivalent root-mean-squares radius of the nucleon density distribution as already reported in details in Refs. [29, 32]. The reduced radius

$r_0 = R/A^{1/3}$ of the equivalent liquid drop model for the parent ($\overline{r_0} = 1.205 \pm 0.001$ fm) and daughter ($\overline{r_0} = 1.206 \pm 0.001$ fm) nuclei is plotted against mass number, A, on the right side in figure 2. The radius-values for the emitted clusters, R_{C}, have been obtained by taking the average of the root-mean-squares radius evaluations of the neutron and proton density distributions such that

$$R_{\mathsf{C}} = \frac{Z}{A} R_{\mathsf{p}} + \left(1 - \frac{Z}{A}\right) R_{\mathsf{n}}, \tag{13}$$

where R_{n} and R_{p} are the smooth descriptions of the neutron and proton radii, respectively, parametrized by Dobaczewski *et al.* [41] as

$$R_{\mathsf{n,p}} = 0.7746 r_0 A^{1/3} \left[1 + \frac{\kappa_1}{A} + \frac{\kappa_2}{A^2} + \left(1 - \frac{2Z}{A}\right)\left(\alpha_1 + \frac{\alpha_2}{A}\right)\right], \tag{14}$$

in which $r_0 = 1.214$ fm, $\kappa_1 = 2.639$, $\kappa_2 = 0.2543$, $\alpha_1 = -0.1233$, and $\alpha_2 = -3.484$ for the proton case, and $r_0 = 1.176$ fm, $\kappa_1 = 3.264$, $\kappa_2 = -0.7121$, $\alpha_1 = 0.1341$, and $\alpha_2 = 4.8280$ for the neutron case. Preliminary calculations have indicated that the small differences between the actual and smooth radius-values (less than $\sim$1.5%) for both the neutron and proton distributions do not affect significantly the evaluated half-life-values for cluster emission cases (not more than a factor 2). In addition, for carbon isotopes a simple extrapolation from the above formalism has been done in estimating their average radius-values. Following the radius parametrization above, the reduced radius for the emitted clusters is plotted on the left side in figure 2 (circles) where a slightly decreasing trend with mass number is apparent.

For the purpose of the present analysis a heavy-fragment nuclear decay (or cluster decay, or radioactive decay by the emission of heavy ions) is the spontaneous nuclear break-up of a parent nucleus of mass number A_{P} into two fragments of mass numbers A_{D} (the daughter, product nuclide) and A_{C} (the emitted fragment, or cluster) such that the corresponding asymmetry defined by

$$\eta = 1 - 2A_{\mathsf{C}}/A_{\mathsf{P}} \tag{15}$$

is in the range $\sim$0.60–0.90 (note that for alpha decay $0.92 \lesssim \eta \lesssim 0.97$, and for fission cases $\eta \lesssim 0.5$).

Finally, the values of angular momentum ℓ have been obtained from the usual nuclear spin ($\boldsymbol{J}$) and parity (π) conservation laws ($\boldsymbol{J}_{\mathsf{P}} = \boldsymbol{J}_{\mathsf{D}} + \boldsymbol{J}_{\mathsf{C}} + \boldsymbol{\ell}$, $\pi_{\mathsf{P}} = \pi_{\mathsf{D}} \cdot \pi_{\mathsf{C}}(-1)^{\ell}$), where

the values of $\boldsymbol{J}$ and π are those reported by Audi *et al.* [37] in their recent compilation of nuclear and decay properties. Last, for the particular cases of $\ell = 0$ one has $x = 0$, and equations (3) and (4) transform, therefore, to

$$G_{\mathsf{ov}} = gH_{\mathsf{ov}}, \quad H_{\mathsf{ov}} = 0.4374703(c-a)\,(\mu_0 Q)^{1/2}\,(z^{-1}-1)^{1/2}, \tag{16}$$

and

$$G_{\mathsf{se}} = 0.62994186 Z_{\mathsf{C}} Z_{\mathsf{D}} \left(\frac{\mu_0}{Q}\right)^{1/2} \cdot \left\{\arccos z^{1/2} - [z(1-z)]^{1/2}\right\}, \quad z^{-1} = 2y\,. \tag{17}$$

3 Systematics of half-life for exotic decays

We have collected a total of 55 measured half-life values for 26 distinct cases of heavy-ion emission from 19 different translead parent nuclei (see table 1). In about half of the cases one has $\ell = 0$, and in the other ones ℓ has taken the values 1, 2, 3, or 4 (5th column in table 1) according to the nuclear spin and parity conservation laws. Q-values for the cluster emission investigated (4th column in table 1) vary from 28.31 MeV (^{226}Ra$\rightarrow^{14}$C) up to 96.78 MeV (^{242}Cm$\rightarrow^{34}$Si), i.e. a small variation of 1.9–2.4 MeV/u in the kinetic energy of the emitted cluster. The partial half-lives, expressed as $\tau_{\mathsf{e}} = \log_{10} T_{1/2}(\mathrm{s})$, are seen in the range $11.0 \lesssim \tau_{\mathsf{e}} \lesssim 27.6$ (6th column in table 1). Of special interest to experimental identification of an emitted heavy-ion in the nuclear decay is its activity relative to alpha activity, namely, the relative branching ratio, B_α (12th column in table 1), the values of which fall on in the range from 5×10^{-17} for the case ^{238}Pu$\rightarrow^{32}$Si decay up to 4×10^{-9} for ^{223}Ra$\rightarrow^{14}$C decay.

Values of the one-parameter, g_{e}, of the present model have been obtained from the experimental half-lives, τ_{e}, and other input data, for all 55 cluster emission cases investigated. It results that the g_{e}-values (8th column in table 1) do not vary significantly neither with the decay case nor the different measurements (when available) for a particular case. Therefore, an average value $\overline{g_{\mathsf{e}}} = 0.260 \pm 0.024$ could be ascribed to the unique parameter of the model, which value showed very adequate at fitting all measured half-life-values. Another method to find the best g-value of the present systematics is to use the radius-data, mass-excess-values, angular momentum, and experimental half-life for all decay cases as input information to

minimize the quantity

$$\sigma = \left\{ \frac{1}{n-2} \sum_{i=1}^{n} \left(\tau_{\mathsf{c}_i} - \tau_{\mathsf{e}_i}\right)^2 \right\}^{1/2} , \quad \tau = \log_{10} T_{1/2} \, , \tag{18}$$

where the subscripts denote experimental (e) or calculated (c) values, and n is the number of cases considered. The preliminary g-value so obtained is then used back into the routine calculation of the model to evaluate the τ_{c_i}-values for the n cases considered initially. Fortunately, in the present analysis none of the 55 cases has been eliminated by the criterion $|\tau_{\mathsf{c}} - \tau_{\mathsf{e}}| \geq 2\sigma$, thus resulting in a final value of $g = 0.259$ with the corresponding $\sigma_{\mathsf{min}} = 0.786$. The process of minimization of σ is shown in Fig. 3, and the best g-value thus obtained compare quite completely with the average $\overline{g_{\mathsf{e}}} = 0.260$ mentioned above (see also Fig. 4-a).

The final, semiempirical parameter-value $g = 0.259$ is then inserted back into the calculation model to evaluate the half-life-values, $\tau_{\mathsf{c}} = \log_{10} T^{\mathsf{c}}_{1/2}$. Results can be appreciated in table 1 (10th column), and they are compared with the experimental ones through the difference $\Delta\tau = \tau_{\mathsf{c}} - \tau_{\mathsf{e}}$ (11th column). The values of the quantity $\Delta\tau$ are found practically distributed normally around $\Delta\tau = 0$ (see the small histogram attached at right in Fig. 4-b), and the width of the $\Delta\tau$-distribution indicates that in 80% of the cases the measured half-life values are reproduced by the present systematics within one order of magnitude. We remark, however, that thirteen measurements, corresponding to eight of the 26 different cases of cluster emission, have been reproduced within a factor 2 (these are the cases No. 1, 2, 14 or 15, 22, 35, 45–48, 51, and 54 or 55 listed in table 1). By far the best agreement between measured and calculated half-life-values is found in the case for $^{234}\mathrm{U}\rightarrow{}^{28}\mathrm{Mg}$ decay (a difference of only 7%!). The greatest differences, on the contrary, are noted for $^{231}\mathrm{Pa}\rightarrow{}^{23}\mathrm{F}$, $^{233}\mathrm{U}\rightarrow{}^{24}\mathrm{Ne}$, and $^{236}\mathrm{U}\rightarrow{}^{30}\mathrm{Mg}$ decay cases. However, they do not exceed ∼1.6 order of magnitude.

In the past, strong correlations between half-life (or decay constant) and the energy of the emitted particle have been established (known as Geiger-Nuttall's plots [72]), originally observed for alpha decay processes in natural radioactivity of heavy elements. The same happens to cluster radioactivity, where quite linear correlations are found between half-life (in a log-scale) and the inverse square root of Q-value for decay of emission cases of a given heavy cluster from nuclides of an isotopic sequence. Thus, complementing the analogy to alpha decay, examples are shown in figures 5–8, where full symbols represent experimental

data, and open ones are calculated values (or predictions) by the present approach. In figure 5 all observed cases for ^{14}C emission have been depicted, and predictions for possible new cases (see section below) are also shown. The only case for oxygen radioactivity observed to date is seen in figure 6 in a comparison with half-life predictions for new oxygen emission cases. Half-lives for radioactivity by the emission of neon isotopes can be appreciated in figure 7, and the decay cases of ^{28}Mg and ^{34}Si emissions from U, Pu, and Cm isotopes are shown in figure 8. In terms of half-life the present systematics covers eighteen orders of magnitude showing good reproducibility to the experimental data.

Finally, according to a modern description of alpha and cluster radioactivity [73, 74], the decay constant for such processes can be written as

$$\lambda = \lambda_0 SP, \quad S = \mathrm{e}^{-G_{\mathsf{ov}}}, \quad P = \mathrm{e}^{-G_{\mathsf{se}}}, \tag{19}$$

where $\lambda_0 = (\sqrt{2}/2)\frac{1}{a}\left(\frac{Q_\alpha}{\mu_0}\right)^{1/2}$ is the usual frequency of assaults on the barrier (cf. equations (1) and (2)), S is the cluster preformation probability at the nuclear surface (also known as the spectroscopic factor), and P is the penetrability factor through the external barrier region ($c \leq s \leq b$ in figure 1). Since the quantity $S = \mathrm{e}^{-G_{\mathsf{ov}}}$ is being given by the penetrability factor through the overlapping region of the barrier ($a \leq s \leq c$ in figure 1) it results that S would correspond to the "arrival" of the cluster (or alpha particle) at the nuclear surface. Values of spectroscopic factor $S = \mathrm{e}^{-G_{\mathsf{ov}}}$ for all decay cases here considered have been calculated, and they are listed in table 1 (9th column) and plotted in figure 4-c. The trend shows a variation by seven orders of magnitude when one passes from ^{34}Si cluster with $S = 10^{-13}$ to ^{14}C cluster with $S = 10^{-6}$.

The values of the quantities S and P are strongly model dependent, and greatly vary also with parameter-values in similar models. The spectroscopic factor contains the structure information of microscopic descriptions to cluster decay processes [73]. According to Poenaru and Greiner [74] the spectroscopic factor corresponds to the "arrival" of the cluster at the nuclear surface (or the preformation probability) which is given by Gamow's factor $\mathrm{e}^{-G_{\mathsf{ov}}}$ calculated in the overlapping region. Table 2 lists λ_0-, S-, and P-values for two examples of cluster emission obtained from five different semiempirical approaches. It is seen that the values for the "knocking frequency" λ_0 do not differ appreciably from each other model (maximum of $\sim$1 order of magnitude), but S and P exhibit differences as high as 5, 7, or even 11 orders of magnitude in the examples shown. However, all models lead practically (within

one order of magnitude) to the same half-life value which reproduces (within a maximum of one order of magnitude) the experimental result. To conclude, inspection on Fig. 4-c reveals that the spectroscopic factor is strongly related to the complexity of the cluster to be preformed, in the sense that a heavy cluster such as ^{14}C is 7 orders of magnitude more easily prompt to escape the nucleus than is ^{34}Si cluster.

4 Half-life predictions for new cluster emission cases

The present routine calculation developed in the precedent sections to half-life evaluations of heavy-ion radioactivities has been used here to make predictions of new possible cases for such exotic decays. The most likely candidates to be experimentally accessed are those that fit Ronen's "gold rule" for cluster radioactivity [27], at the same time that the expected branching ratio relative to alpha decay, B_α, be not lower than about 10^{-16}, i.e. the limiting B_α-value which still allows detection, by the current experimental techniques, of heavy nuclear fragments emitted in the presence of an intense alpha-particle background. By using the criteria mentioned above 30 new cases for exotic decays not yet observed experimentally have been found with half-life predictions given in table 3 (6th column). Comparison with half-life evaluations by Poenaru *et al.* [16, 17] (8th column), and in a few cases with the ones by Kuklin *et al.* [25] (7th column), is also shown. In the latter case, significant differences (up to four orders of magnitude) are noted, but these differences become smaller (or even null) when comparing the present half-life evaluations with those reported in [16, 17]. Table 3 shows in addition that new clusters (not yet detected in radioactive decay) such as ^{12}C, ^{15}N, ^{16}O, ^{18}O, and ^{29}Mg are also good candidates to exotic radioactivity. Of special attention in table 3 are the cases No. 6, 16, and 21–23, for, if eventually detected, they could be considered the most interesting cases of *natural* cluster radioactivity. It should be remarked that since the mass-excess for ^{204}Pt isotope is not available from the current mass table by Audi *et al.* [37], its value has been taken from the mass prediction by Möller *et al.* [40], therefore the corresponding half-life prediction for the decay $^{238}\mathrm{U}\rightarrow{}^{204}\mathrm{Pt}+{}^{34}\mathrm{Si}$ may still contain uncertainties to some extent. Finally, examples of half-life predictions in comparison with decay cases already observed are depicted for ^{14}C emission from Fr, Ra, Ac, and Th isotopes (figure 5), ^{16,18,20}O from Th isotopes (figure 6), and ^{28}Mg and ^{34}Si cluster emissions from U, Np, Pu, and Cm isotopes (figure 8).

5 Uncertainties to calculated half-lives

The calculated half-life, expressed as $\tau_{\mathsf{c}} = \log_{10} T^{\mathsf{c}}_{1/2}(\mathrm{s})$, depends basically upon the radius- and mass-excess-values adopted for the nuclides, angular momentum ℓ of the transition, and the value found semiempirically for the unique parameter of the model, g, such that, formally,

$$\tau = f(R_i, \Delta M_i, \ell, g) \tag{20}$$

where $i = \mathsf{P}$ (parent nucleus), D (daughter product nucleus), and C (emitted cluster). Although all these quantities are subject to uncertainties, preliminary calculations have indicated that by far the most significant contributions to the final uncertainty in the calculated half-life, $\delta\tau_{\mathsf{c}}$, come from the uncertainties associated to the radius-value of the emitted cluster, δR_{C}, and that of parameter g, $\delta g = 0.024$, this latter being thirty times more significant than the former one. Therefore, $\delta\tau_{\mathsf{c}}$ can be evaluated by

$$\delta\tau_{\mathsf{c}} = \left[\left(\frac{\partial f}{\partial R_{\mathsf{C}}} \right)^2 (\delta R_{\mathsf{C}})^2 + \left(\frac{\partial f}{\partial g} \right)^2 (\delta g)^2 \right]^{1/2} . \tag{21}$$

Now, the uncertainty associated to the cluster radius can be estimated as

$$\delta R_{\mathsf{C}} = \frac{Z_{\mathsf{C}}}{A_{\mathsf{C}}} \cdot \Delta r_{\mathsf{p}} + \left(1 - \frac{Z_{\mathsf{C}}}{A_{\mathsf{C}}} \right) \cdot \Delta r_{\mathsf{n}} \,, \tag{22}$$

where Δr_{p} and Δr_{n} are the differences between the actual radius and the smooth description of the radius-value for the proton and neutron, respectively, following the radius parametrization by Dobaczewski *et al.* [41] (see section 2, equation (14)). In this way, values of δR_{C} have been estimated as 0.02 fm for ^{22}Ne, ^{30}Mg, and ^{32}Si, 0.03 fm for ^{20}O, ^{23}F, and ^{34}Si, and 0.04 fm for ^{14}C, $^{24–26}$Ne, and ^{28}Mg clusters. Finally, one obtained for the uncertainties associated to the predicted (or calculated) half-life values which do not exceed approximately one order of magnitude (see 10th column in table 1, and 7th column in table 3).

6 Final remarks and conclusion

A semiempirical, one-parameter model developed recently to systematize measured half-life values and to predict for new ones of alpha decay processes [29, 31, 32] has been extended

here to analyse in a systematic way all available half-life data for cluster (or exotic) decays. The analogy to alpha decay is quite complete, but some quantitative differences should be remarked such as *i*) a substantial broader overlapping region of fragments thus making cluster preformation probability at the nuclear surface 4 to 10 orders of magnitude smaller than that for an alpha particle; *ii*) the rarety of the cluster emission processes which is evidenced by an extremely small branching ratio relative to alpha decay ($10^{-17} \lesssim B_\alpha \lesssim 10^{-9}$); *iii*) since such a case of radioactive decay is not easy of being experimentally identified the uncertainties to measured half-lives are in general large, and, therefore, the standard deviation from semiempirical treatments of the data is intrinsically greater than that obtained in alpha decay; *iv*) half-life predictions for new cases of cluster decay are consequently valid within, at best, one order of magnitude or so; *v*) the present analysis has shown in addition that for translead parent nuclei up to curium isotopes the only possible cases of rare radioactivity to occur are (or may be) those for the emission of ^{12,14}C, ^{15}N, ^{16,18,20}O, ^{23}F, ^{22,24,25,26}Ne, $^{28–30}$Mg, and ^{32,34}Si clusters; *vi*) the best chance for heavy-ion emission to take place spontaneously is for those cases where the daughter nucleus has a magic structure, in the vicinity of ^{208}Pb.

Geiger-Nuttall's plots for different heavy-ion emission cases emerge nicely, therefore showing that cluster radioactivity could be successfully described by the current quantum-mechanical tunnelling mechanism of penetration through a potential barrier.

The present analysis allowed us to make half-life predictions for a number of new cases of heavy-ion radioactivities. Particularly, it would be very important and interesting as well to see detected in a future the cases for *natural* cluster radioactivity such as ^{14}C from ^{223}Ac ($B_\alpha \sim 2 \times 10^{-11}$), ^{26}Ne from ^{232}Th ($B_\alpha \sim 3 \times 10^{-12}$), ^{28,29}Mg from ^{235}U ($B_\alpha \sim 10^{-12}$), or, at least, the intriguing case for emission of ^{34}Si from ^{238}U, for which B_α is evaluated in the range 10^{-13}–10^{-11}. It would be worthwhile if all these possible disintegration processes of measurable half-lives could be investigated taking advantage of the present and/or novel experimental techniques. The ^{238}U$\rightarrow^{34}$Si radioactive decay process represents indeed a challenge to experimental research groups.

To conclude, the authors recall that the possibility for this new type of radioactivity (spontaneous emission of nuclear clusters heavier than the alpha particle) to occur was quantitatively investigated for the first time in 1975 by de Carvalho and co-workers [6, 7, 10]. Despite the incompatibility of their results with what is nowadays known about, they

nonetheless launched into the basic ideas and furnished the motivation for investigating such new and exciting mode of nuclear disintegration process.

References

[1] Rose H J and Jones G A 1984 *Nature* (London) **307** 245

[2] Aleksandrov D V, Belyatskĭi A F, Glukhov Yu A, Nikol'skĭi E Yu, Novatskĭi B G, Ogloblin A A and Stepanov D N 1984 *Pis'ma Zh. Eksp. Teor. Fiz.* **40** 152 [1984 *Soviet Physics JETP Lett.* **40** 909]

[3] Gales S, Hourani E, Hussonnois M, Schapira J P, Stab L and Vergnes M 1984 *Phys. Rev. Lett.* **53** 759

[4] Price P B, Stevenson J D, Barwick S W and Ravn H L 1985 *Phys. Rev. Lett.* **54** 297

[5] Kutschera W, Ahmad I, Armato III S G, Friedman A M, Gindler J E, Henning W, Ishii T, Paul M and Rehm K E 1985 *Phys. Rev. C* **32** 2036

[6] de Carvalho H G, Martins J B, de Souza I O and Tavares O A P 1975 *An. Acad. brasil. Ciênc.* **47** 567

[7] de Carvalho H G, Martins J B, de Souza I O and Tavares O A P 1976 *An. Acad. brasil. Ciênc.* **48** 205

[8] de Souza I O 1975 Sep. *Ms. Thesis* Centro Brasileiro de Pesquisas Físicas - CBPF

[9] Tavares O A P 1978 Dec. *Doctoral Thesis* Centro Brasileiro de Pesquisas Físicas - CBPF

[10] de Carvalho H G, Martins J B and Tavares O A P 1986 *Phys. Rev. C* **34** 2261

[11] Săndulescu A and Greiner W 1977 *J. Phys. G: Nucl. Part. Phys.* **3** L189

[12] Săndulescu A, Lustig H J, Hahn J and Greiner W 1978 *J. Phys. G: Nucl. Part. Phys.* **4** L279

[13] Săndulescu A, Poenaru D N and Greiner W 1980 *Fiz. Elem. Chastits At. Yadra* **11** 1334 [1980 *Sov. J. Part. Nucl.* **11** 528]

[14] Poenaru D N, Ivascu M, Săndulescu A and Greiner W 1984 *J. Phys. G: Nucl. Part. Phys.* **10** L183

[15] Poenaru D N, Ivascu M, Săndulescu A and Greiner W 1985 *Phys. Rev. C* **32** 572

[16] Poenaru D N, Greiner W, Depta K, Ivascu M, Mazilu D and Săndulescu A 1986 *At. Data Nucl. Data Tables* **34** 423

[17] Poenaru D N, Schnabel D, Greiner W, Mazilu D and Gherghescu R 1991 *At. Data Nucl. Data Tables* **48** 231

[18] Zamyatnin Yu S, Mikheev V L, Tretyakova S P and Furman V I 1990 *Fiz. Elem. Chastits At. Yadra* **21** 537 [1990 *Sov. J. Part. Nucl.* **21** 231]

[19] Gonçalves M and Duarte S B 1993 *Phys. Rev. C* **48** 2409

[20] Guglielmetti A, Bonetti R, Poli G, Price P B, Westphol A J, Janas Z, Keller H, Kirchner R, Kepller O, Piechaczek A, Roeckl E, Schimidt K, Plochocki A, Szerypo J and Blank B 1995 *Phys. Rev. C* **52** 740

[21] Ardisson G and Hussonnois M 1995 *Radioch. Acta* **70/71** 123

[22] Poenaru D N (Ed.) 1996 *Nuclear Decay Modes* (Institute of Physics Publishing, Bristol, UK) Chapters 6–9

[23] Tretyakova S P, Ogloblin A A and Pik-Pichak G A 2003 *Phys. Atom. Nucl.* **66** 1618

[24] Kuklin S N, Adamian G G and Antonenko N V 2005 *Phys. Atom. Nucl.* **68** 1443

[25] Kuklin S N, Adamian G G and Antonenko N V 2005 *Phys. Rev. C* **71** 014301

[26] Hourani E, Hussonnois M and Poenaru D N 1989 *Ann. Phys.* (Paris) **14** 311

[27] Ronen Y 1991 *Phys. Rev. C* **44** R594

[28] Duarte S B, Tavares O A P, Guzmán F, Dimarco A, García F, Rodriguez O and Gonçalves M 2002 *At. Data Nucl. Data Tables* **80** 235

[29] Tavares O A P, Medeiros E L and Terranova M L 2005 *J. Phys. G: Nucl. Part. Phys.* **31** 129

[30] de Marcillac P, Coron N, Dambier G, Leblanc J and Moalic J P 2003 *Nature* (London) **422** 876

[31] Tavares O A P, Terranova M L and Medeiros E L 2006 *Nucl. Instrum. Meth. Phys. Res. B* **243** 256

[32] Medeiros E L, Rodrigues M M N, Duarte S B and Tavares O A P 2006 *J. Phys. G: Nucl. Part. Phys.* **32** B23

[33] Tavares O A P and Terranova M L 1997 *Radiat. Meas.* **27** 19

[34] Medeiros E L, Rodrigues M M N, Duarte S B and Tavares O A P 2006 *J. Phys. G: Nucl. Part. Phys.* **32** 2345

[35] Danevich F A *et al.* 2003 *Phys. Rev. C* **67** 014310

[36] Zdesenko Yu G, Avignone III F T, Brudanin V B, Danevich F A, Nagorny S S, Solsky I M and Tretyak V I 2005 *Nucl. Instrum. Methods Phys. Res. A* **538** 657

[37] Audi G, Bersillon O, Blachot J and Wapstra A H 2003 *Nucl. Phys. A* **729** 3

[38] Huang K-N, Aoyagi M, Chen M H, Crasemann B and Mark H 1976 *At. Data Nucl. Data Tables* **18** 243

[39] Myers W D 1977 *Droplet Model of Atomic Nuclei* (New York: Plenum)

[40] Möller P, Nix J R, Myers W D and Swiatecki W J 1995 *At. Data Nucl. Data Tables* **59** 185

[41] Dobaczewski J, Nazarewicz W and Werner T R 1996 *Z. Phys. A* **354** 27

[42] Bonetti R, Chiesa C, Guglielmetti A, Migliorino C, Monti P, Pasinetti A L and Ravn H L 1994 *Nucl. Phys.* A **576** 21

[43] Hussonnois M, Le Du J F, Brillard L, Dalmasso J and Ardisson G 1991 *Phys. Rev. C* **43** 2599

[44] Hourani E, Hussonnois M, Stab L, Brillard L, Gales S and Schapira J P 1985 *Phys. Lett. B* **160** 375

[45] Hourani E, Berrier-Ronsin G, Elayi A, Hoffmann-Rothe P, Mueller A C, Rosier L, Rotbard G, Renou G, Lièbe A, Poenaru D N and Ravn H L 1995 *Phys. Rev. C* **52** 267

[46] Brillard L, Elayi A G, Hourani E, Hussonnois M, Le Du J F, Rosier L H and Stab L 1989 *Compt. Rend. Acad. Sci.* (Paris) **309** 1105

[47] Barwick S W, Price P B, Ravn H L, Hourani E and Hussonnois M 1986 *Phys. Rev. C* **34** 362

[48] Bonetti R, Chiesa C, Guglielmetti A, Matheoud R, Migliorino C, Pasinetti A L and Ravn H L 1993 *Nucl. Phys. A* **562** 32

[49] Guglielmetti A, Bonetti R, Ardisson G, Barci V, Giles T, Hussonnois M, Le Du J F, Le Naour C, Mikheev V L, Pasinetti A L, Ravn H L, Tretyakova S P and Trubert D 2001 *Eur. Phys. J. A* **12** 383

[50] Bonetti R, Chiesa C, Guglielmetti A, Migliorino C, Cesana A and Terrani M 1993 *Nucl. Phys. A* **556**, 115

[51] Price P B, Bonetti R, Guglielmetti A, Chiesa C, Matheoud R, Migliorino C and Moody K J 1992 *Phys. Rev. C* **46** 1939

[52] Bonetti R, Carbonini C, Guglielmetti A, Hussonnois M, Trubert D and Le Naour C 2001 *Nucl. Phys. A* **686** 64

[53] Qiangyan P, Weifan Y, Shuanggui Y, Zongwei L, Taotao M, Yixiao L, Dengming K, Jimin Q, Zihua L, Mutian Z and Shuhong W 2000 *Phys. Rev. C* **62** 044612

[54] Tretyakova S P, Săndulescu A, Mikheev V L, Hasegan D, Lebedev I A, Zamyatnin Yu S, Korotkin Yu S and Myasoedov B F 1985 *JINR - Rapid Communications* **13** 34

[55] Săndulescu A, Zamyatnin Yu S, Lebedev I A, Myasoedov B F, Tretyakova S P and Hasegan D 1984 *JINR - Rapid Communications* **5** 5

[56] Tretyakova S P, Săndulescu A, Mikheev V L, Zamyatnin Yu S, Lebedev I A, Myasoedov B F, Khashegan D and Korotkin Yu S 1986 *Bull. Acad. Sci. USSR, Phys. Ser.* **50** 52

[57] Ronen Y 2002 *Ann. Nucl. Energy* **29** 1013

[58] Barwick S W, Price P B and Stevenson J D 1985 *Phys. Rev. C* **31** 1984

[59] Bonetti R, Fioretto E, Migliorino C, Pasinetti A, Barranco F, Vigezzi E and Broglia R A 1990 *Phys. Lett. B* **241** 179

[60] Bonetti R, Chiesa C, Guglielmetti A, Migliorino C, Cesana A, Terrani M and Price P B 1991 *Phys. Rev. C* **44** 888

[61] Tretyakova S P, Săndulescu A, Zamyatnin Yu S, Korotkin Yu S and Mikheev V L 1985 *JINR - Rapid Communications* **7** 23

[62] Price P B, Moody K J, Hulet E K, Bonetti R and Migliorino C 1991 *Phys. Rev. C* **43** 1781

[63] Wang S, Price P B, Barwick S W, Moody K J and Hulet E K 1987 *Phys. Rev. C* **36** 2717

[64] Tretyakova S P, Zamyatnin Yu S, Kovantsev V N, Korotkin Yu S, Mikheev V L, and Timofeev G A 1989 *Z. Phys. A* **333** 349

[65] Price P B 1989 in *Proc. Int. Conf. on Fifty Years of Research in Nuclear Fission* (West Berlin)

[66] Ogloblin A A, Venikov N I, Lisin S K, Pirozhkov S V, Pchelin V A, Rodionov Yu F, Semochkin V M, Shabrov V A, Shvetsov I K, Shubko V M, Tretyakova S P and Mikheev V L 1990 *Phys. Lett. B* **235**, 35

[67] Hussonnois M, Le Du J F, Trubert D, Bonetti R, Guglielmetti A, Guzel T, Tretyakova S P, Mikheev V L, Golovchenko A N and Ponomarenko V A 1995 *JETP Lett.* **62** 701

[68] Wang S, Snowden-Ifft D, Price P B, Moody K J and Hulet E K 1989 *Phys. Rev. C* **39** R1647

[69] Tretyakova S P, Mikheev V L, Ponomarenko V A, Golovchenko A N, Ogloblin A A and Shigin V A 1994 *JETP Lett.* **59** 394

[70] Tretyakova S P, Bonetti R, Golovchenko A, Guglielmetti A, Ilic R, Mazzocchi Ch, Mikheev V, Ogloblin A, Ponomarenko V, Shigin V and Skvar J 2001 *Radiat. Measurem.* **34** 241

[71] Ogloblin A A, Bonetti R, Denisov V A, Guglielmetti A, Itkis M G, Mazzocchi C, Mikheev V L, Oganessian Yu Ts, Pik-Pichak G A, Poli G, Pirozhkov S M, Semochkin V M, Shigin V A, Shvetsov I K and Tretyakova S P 2000 *Phys. Rev. C* **61** 034301

[72] Geiger H and Nuttall J M 1911 *Phil. Mag.* **22** 613; Geiger H 1921 *Z. Phys.* **8** 45

[73] Blendowske R, Fliessbach T and Walliser H 1991 *Z. Phys. A* **339** 121

[74] Poenaru D N and Greiner W 1991 *Phys. Scr.* **44** 427

Table 1 - Comparison between experimental and present calculated half-life-values for known radioactive decay cases by the emission of heavy nuclear fragments[a].

			Experimental decay data								
		Asymmetry[b]	Q-value[c]					Calculated data		Difference	
No.	Decay case	η	(MeV)	ℓ	τ_e	Ref.	g_e	S^d	τ_c	$\Delta\tau = \tau_c - \tau_e$	B_α^e
1	$^{221}\mathrm{Fr} \rightarrow {}^{14}\mathrm{C} + {}^{207}\mathrm{Tl}$	0.873	31.400	3	14.52	[42]	0.265	1.1(−6)	14.39 ± 0.56	−0.13	1.2(−12)
2	$^{221}\mathrm{Ra} \rightarrow {}^{14}\mathrm{C} + {}^{207}\mathrm{Pb}$	0.873	32.506	3	13.38	[42]	0.265	1.1(−6)	13.26 ± 0.56	−0.12	1.6(−12)
3	$^{222}\mathrm{Ra} \rightarrow {}^{14}\mathrm{C} + {}^{208}\mathrm{Pb}$	0.874	33.160	0	11.01	[4]	0.225	1.3(−6)	11.80 ± 0.56	0.79	6.0(−11)
4					11.21	[43]	0.233			0.59	
5					11.08	[44]	0.228			0.72	
6	$^{223}\mathrm{Ra} \rightarrow {}^{14}\mathrm{C} + {}^{209}\mathrm{Pb}$	0.874	31.939	4	15.21	[4]	0.295	1.0(−6)	14.38 ± 0.50	−0.83	4.1(−9)
7					15.06	[1]	0.289			−0.68	
8					15.11	[2]	0.291			−0.73	
9					15.25	[3]	0.297			−0.87	
10					15.32	[5]	0.300			−0.94	
11					15.04	[45]	0.288			−0.66	
12					15.19	[46]	0.294			−0.81	
13	$^{224}\mathrm{Ra} \rightarrow {}^{14}\mathrm{C} + {}^{210}\mathrm{Pb}$	0.875	30.646	0	15.87	[4]	0.233	8.6(−7)	16.48 ± 0.57	0.61	1.0(−11)
14	$^{226}\mathrm{Ra} \rightarrow {}^{14}\mathrm{C} + {}^{212}\mathrm{Pb}$	0.876	28.307	0	21.20	[44]	0.248	5.9(−7)	21.46 ± 0.59	0.26	1.7(−11)
15					21.24	[47]	0.250			0.22	
16	$^{225}\mathrm{Ac} \rightarrow {}^{14}\mathrm{C} + {}^{211}\mathrm{Bi}$	0.876	30.588	4	17.16	[48]	0.227	7.0(−7)	17.92 ± 0.58	0.76	1.0(−12)
17					17.28	[49]	0.232			0.64	
18	$^{228}\mathrm{Th} \rightarrow {}^{20}\mathrm{O} + {}^{208}\mathrm{Pb}$	0.825	44.872	0	20.72	[50]	0.223	4.9(−9)	21.90 ± 0.78	1.18	7.6(−15)
19	$^{231}\mathrm{Pa} \rightarrow {}^{23}\mathrm{F} + {}^{208}\mathrm{Pb}$	0.801	52.013	1	26.02	[51]	0.300	3.8(−10)	24.53 ± 0.88	−1.49	3.0(−13)
20	$^{230}\mathrm{U} \rightarrow {}^{22}\mathrm{Ne} + {}^{208}\mathrm{Pb}$	0.809	61.577	0	19.57	[52]	0.227	5.5(−10)	20.72 ± 0.86	1.15	3.5(−15)
21					20.15	[53]	0.243			0.57	
22	$^{230}\mathrm{Th} \rightarrow {}^{24}\mathrm{Ne} + {}^{206}\mathrm{Hg}$	0.791	57.943	0	24.63	[54]	0.252	1.3(−10)	24.92 ± 0.93	0.29	2.9(−13)
23	$^{231}\mathrm{Pa} \rightarrow {}^{24}\mathrm{Ne} + {}^{207}\mathrm{Tl}$	0.792	60.596	1	23.23	[55]	0.286	1.8(−10)	22.25 ± 0.92	−0.98	5.7(−11)
24					22.89	[51]	0.276			−0.64	
25					23.43	[56]	0.291			−1.18	
26					23.38[f]	—	0.289			−1.13	
27					22.72[g]	—	0.272			−0.47	
28	$^{232}\mathrm{U} \rightarrow {}^{24}\mathrm{Ne} + {}^{208}\mathrm{Pb}$	0.793	62.499	0	21.34	[58]	0.275	2.0(−10)	20.76 ± 0.91	−0.58	3.7(−12)
29					20.41	[59]	0.250			0.35	
30					20.39	[60]	0.249			0.37	
31	$^{233}\mathrm{U} \rightarrow {}^{24}\mathrm{Ne} + {}^{209}\mathrm{Pb}$	0.794	60.674	2	24.84	[61]	0.297	1.4(−10)	23.40 ± 0.93	−1.44	2.0(−11)
32					24.85	[62]	0.297			−1.45	
33	$^{234}\mathrm{U} \rightarrow {}^{24}\mathrm{Ne} + {}^{210}\mathrm{Pb}$	0.795	59.015	0	25.07	[63]	0.241	1.0(−10)	25.79 ± 0.94	0.72	1.2(−13)
34					25.30	[64]	0.247			0.49	
35					25.93	[60]	0.263			−0.14	
36	$^{235}\mathrm{U} \rightarrow {}^{24}\mathrm{Ne} + {}^{211}\mathrm{Pb}$	0.796	57.552	1	27.44	[60]	0.243	7.5(−11)	28.08 ± 0.95	0.64	1.8(−12)
37	$^{233}\mathrm{U} \rightarrow {}^{25}\mathrm{Ne} + {}^{208}\mathrm{Pb}$	0.785	60.965	2	24.84	[61]	0.289	7.9(−11)	23.69 ± 0.95	−1.15	1.0(−11)
38					24.85	[62]	0.289			−1.16	
39	$^{235}\mathrm{U} \rightarrow {}^{25}\mathrm{Ne} + {}^{210}\mathrm{Pb}$	0.787	57.945	3	27.44	[60]	0.236	4.2(−11)	28.35 ± 0.98	0.91	9.7(−13)
40	$^{234}\mathrm{U} \rightarrow {}^{26}\mathrm{Ne} + {}^{208}\mathrm{Pb}$	0.778	59.653	0	25.07	[63]	0.230	3.3(−11)	26.27 ± 0.99	1.20	4.1(−14)

			Experimental decay data								
		Asymmetry[b]	Q-value[c]					Calculated data		Difference	
No.	Decay case	η	(MeV)	ℓ	τ_{e}	Ref.	g_{e}	S^{d}	τ_{c}	$\Delta\tau = \tau_{\mathsf{c}} - \tau_{\mathsf{e}}$	B_α^{e}
41					25.93	[60]	0.251			0.34	
42					25.89	[60]	0.250			0.38	
43					25.30	[64]	0.235			0.97	
44	$^{235}\mathrm{U} \to {}^{26}\mathrm{Ne} + {}^{209}\mathrm{Pb}$	0.779	58.293	1	27.44	[60]	0.235	2.5(−11)	28.42 ± 1.00	0.98	8.2(−13)
45	$^{234}\mathrm{U} \to {}^{28}\mathrm{Mg} + {}^{206}\mathrm{Hg}$	0.761	74.332	0	25.54	[63]	0.260	4.6(−12)	25.50 ± 1.07	−0.04	2.4(−13)
46					25.73	[65]	0.265			−0.23	
47					25.70[g]	—	0.264			−0.20	
48					25.53	[64]	0.260			−0.03	
49	$^{236}\mathrm{Pu} \to {}^{28}\mathrm{Mg} + {}^{208}\mathrm{Pb}$	0.763	79.899	0	21.65	[66]	0.271	7.9(−12)	21.17 ± 1.05	−0.48	6.0(−14)
50					21.52	[67]	0.268			−0.35	
51	$^{238}\mathrm{Pu} \to {}^{28}\mathrm{Mg} + {}^{210}\mathrm{Pb}$	0.765	76.140	0	25.69	[68]	0.256	3.6(−12)	25.83 ± 1.08	0.14	
52	$^{236}\mathrm{U} \to {}^{30}\mathrm{Mg} + {}^{206}\mathrm{Hg}$	0.746	72.524	0	27.58	[69]	0.225	9.8(−13)	29.16 ± 1.12	1.58	5.3(−15)
53	$^{238}\mathrm{Pu} \to {}^{32}\mathrm{Si} + {}^{206}\mathrm{Hg}$	0.731	91.452	0	25.30	[68]	0.250	2.0(−13)	25.74 ± 1.18	0.44	5.0(−17)
54	$^{242}\mathrm{Cm} \to {}^{34}\mathrm{Si} + {}^{208}\mathrm{Pb}$	0.719	96.781	0	23.15	[70]	0.254	1.0(−13)	23.43 ± 1.22	0.28	5.2(−17)
55					23.15	[71]	0.254			0.28	

[a] In the 6th and 10th columns the half-life is represented by $\tau = \log T_{1/2}(\mathrm{s})$.

[b] See equation (15).

[c] Screening effects included (see equation (12)).

[d] Spectroscopic factor, $S = \mathrm{e}^{-G_{\mathsf{ov}}}$, where G_{ov} is given by equation (3).

[e] Branching ratio relative to alpha decay.

[f] Quoted in [51].

[g] Quoted in [57].

Table 2 - Comparison between different models in evaluating the quantities λ_0, S, and P of the decay rate $\lambda = \lambda_0 SP$ (eq. (19)) to calculate the associated half-life $\tau_c = \log[(\ln 2)/\lambda]$ for two heavy-ion emission cases.

Author	$^{228}\mathrm{Th} \rightarrow {}^{20}\mathrm{O} + {}^{208}\mathrm{Pb}$, $\tau_e = 20.72$[a]				$^{242}\mathrm{Cm} \rightarrow {}^{34}\mathrm{Si} + {}^{208}\mathrm{Pb}$, $\tau_e = 23.15$[b]			
and Reference	λ_0 (s^{-1})	S	P	τ_c	λ_0 (s^{-1})	S	P	τ_c
Blendowske *et al.* [73]	3.27×10^{21}	1.15×10^{-14}	2.83×10^{-30}	21.81	3.18×10^{21}	6.20×10^{-25}	8.45×10^{-23}	24.62
Poenaru and Greiner [74]	1.02×10^{22}	4.34×10^{-12}	1.93×10^{-33}	21.91	1.02×10^{22}	1.84×10^{-20}	4.10×10^{-27}	23.95
Kuklin *et al.* [24] (deformation included)	5.80×10^{20}	2.90×10^{-14}	7.70×10^{-29}	20.73	5.80×10^{20}	1.5×10^{-23}	1.5×10^{-21}	22.73
Kuklin *et al.* [24] (spherical approx.)	5.80×10^{20}	1.5×10^{-11}	1.5×10^{-31}	20.73	5.80×10^{20}	1.5×10^{-20}	1.5×10^{-24}	22.73
This work	2.45×10^{21}	5.04×10^{-9}	7.22×10^{-36}	21.90	2.99×10^{21}	1.03×10^{-13}	8.23×10^{-33}	23.43

[a] Ref. [50]

[b] Ref. [70]

Table 3 - Half-life predictions for the most probable exotic radioactive decay cases not yet observed experimentally.

No.	Decay case	Asymmetry η	Q-value[a] (MeV)	ℓ	Spectroscopic factor, S[b]	Half-life values, $\tau = \log_{10} T_{1/2}(\mathrm{s})$ This work	Ref. [25]	Ref. [17]	Branching ratio to alpha decay
1	$^{222}\mathrm{Fr} \rightarrow {}^{14}\mathrm{C} + {}^{208}\mathrm{Tl}$	0.874	30.187	3	8.7(−7)	16.76 ± 0.57	—	18.2	1.5(−14)
2	$^{223}\mathrm{Fr} \rightarrow {}^{14}\mathrm{C} + {}^{209}\mathrm{Tl}$	0.874	29.110	1	7.5(−7)	18.79 ± 0.58	—	19.0	2.1(−16)
3	$^{220}\mathrm{Ra} \rightarrow {}^{12}\mathrm{C} + {}^{208}\mathrm{Pb}$	0.891	32.132	0	3.9(−6)	11.43 ± 0.51	14.40	10.5	6.6(−14)
4	$^{225}\mathrm{Ra} \rightarrow {}^{14}\mathrm{C} + {}^{211}\mathrm{Pb}$	0.875	29.576	4	6.8(−7)	19.06 ± 0.58	—	20.0	1.1(−13)
5	$^{222}\mathrm{Ac} \rightarrow {}^{12}\mathrm{C} + {}^{210}\mathrm{Bi}$	0.892	31.525	0	3.1(−6)	13.31 ± 0.52	—	14.7	2.4(−13)
6	$^{223}\mathrm{Ac} \rightarrow {}^{14}\mathrm{C} + {}^{209}\mathrm{Bi}$	0.874	33.177	2	1.1(−6)	12.75 ± 0.56	—	12.7	2.2(−11)
7	$^{224}\mathrm{Ac} \rightarrow {}^{15}\mathrm{N} + {}^{209}\mathrm{Pb}$	0.866	37.877	4	2.3(−7)	17.30 ± 0.62	—	18.7	5.5(−13)
8	$^{227}\mathrm{Ac} \rightarrow {}^{14}\mathrm{C} + {}^{213}\mathrm{Bi}$	0.877	28.174	4	4.8(−7)	23.17 ± 0.59	—	23.1	4.6(−15)
9	$^{223}\mathrm{Th} \rightarrow {}^{16}\mathrm{O} + {}^{207}\mathrm{Pb}$	0.856	46.724	3	8.1(−8)	15.61 ± 0.66	—	16.6	1.5(−16)
10	$^{224}\mathrm{Th} \rightarrow {}^{14}\mathrm{C} + {}^{210}\mathrm{Pb}$	0.875	33.043	0	9.6(−7)	13.75 ± 0.56	15.83	13.1	1.8(−14)
11	$^{225}\mathrm{Th} \rightarrow {}^{16}\mathrm{O} + {}^{209}\mathrm{Pb}$	0.858	44.810	4	5.9(−8)	18.58 ± 0.67	—	18.8[c]	1.5(−16)
12	$^{226}\mathrm{Th} \rightarrow {}^{18}\mathrm{O} + {}^{208}\mathrm{Pb}$	0.841	45.876	0	2.1(−8)	18.51 ± 0.72	16.49	18.0	5.7(−16)
13	$^{227}\mathrm{Th} \rightarrow {}^{14}\mathrm{C} + {}^{213}\mathrm{Pb}$	0.877	29.553	4	5.2(−7)	21.04 ± 0.58	—	22.0	1.5(−15)
14	$^{227}\mathrm{Th} \rightarrow {}^{18}\mathrm{O} + {}^{209}\mathrm{Pb}$	0.841	44.351	4	1.5(−8)	21.29 ± 0.73	—	22.6	8.5(−16)
15	$^{229}\mathrm{Th} \rightarrow {}^{20}\mathrm{O} + {}^{209}\mathrm{Pb}$	0.825	43.552	2	3.8(−9)	24.31 ± 0.79	—	26.1	1.2(−13)
16	$^{232}\mathrm{Th} \rightarrow {}^{26}\mathrm{Ne} + {}^{206}\mathrm{Hg}$	0.776	56.146	0	2.7(−11)	29.24 ± 0.98	—	29.4[c]	2.6(−12)
17	$^{225}\mathrm{Pa} \rightarrow {}^{15}\mathrm{N} + {}^{210}\mathrm{Po}$	0.867	40.326	2	2.6(−7)	14.88 ± 0.62	—	14.8	2.2(−15)
18	$^{225}\mathrm{Pa} \rightarrow {}^{16}\mathrm{O} + {}^{209}\mathrm{Bi}$	0.858	47.487	2	7.9(−8)	15.34 ± 0.66	—	15.3	7.8(−16)
19	$^{226}\mathrm{U} \rightarrow {}^{16}\mathrm{O} + {}^{210}\mathrm{Po}$	0.858	48.173	0	7.5(−8)	15.23 ± 0.67	—	14.5	1.6(−16)
20	$^{233}\mathrm{U} \rightarrow {}^{28}\mathrm{Mg} + {}^{205}\mathrm{Hg}$	0.760	74.446	3	4.6(−12)	25.54 ± 1.07	22.92	27.4	1.4(−13)
21	$^{235}\mathrm{U} \rightarrow {}^{28}\mathrm{Mg} + {}^{207}\mathrm{Hg}$	0.762	72.380	1	3.1(−12)	28.15 ± 1.08	—	27.3[c]	1.6(−12)
22	$^{235}\mathrm{U} \rightarrow {}^{29}\mathrm{Mg} + {}^{206}\mathrm{Hg}$	0.753	72.706	3	1.8(−12)	28.45 ± 1.10	26.78	27.4[c]	7.9(−13)
23	$^{238}\mathrm{U} \rightarrow {}^{34}\mathrm{Si} + {}^{204}\mathrm{Pt}$	0.714	86.062	0	4.4(−14)	30.22 ± 1.25	—	28.0[c]	8.3(−14)
24	$^{235}\mathrm{Np} \rightarrow {}^{28}\mathrm{Mg} + {}^{207}\mathrm{Tl}$	0.762	77.322	2	6.2(−12)	23.07 ± 1.05	—	24.0	2.8(−16)
25	$^{236}\mathrm{Np} \rightarrow {}^{28}\mathrm{Mg} + {}^{208}\mathrm{Tl}$	0.763	75.373	1	4.2(−12)	25.50 ± 1.07	—	28.1	1.5(−13)
26	$^{237}\mathrm{Np} \rightarrow {}^{30}\mathrm{Mg} + {}^{207}\mathrm{Tl}$	0.747	75.043	2	1.2(−12)	27.15 ± 1.11	—	28.3	4.8(−14)
27	$^{239}\mathrm{Pu} \rightarrow {}^{34}\mathrm{Si} + {}^{205}\mathrm{Hg}$	0.715	91.095	1	5.9(−14)	27.16 ± 1.23	—	29.0	5.1(−16)
28	$^{240}\mathrm{Pu} \rightarrow {}^{34}\mathrm{Si} + {}^{206}\mathrm{Hg}$	0.717	91.291	0	6.4(−14)	26.83 ± 1.23	—	27.4	3.1(−16)
29	$^{241}\mathrm{Am} \rightarrow {}^{34}\mathrm{Si} + {}^{207}\mathrm{Tl}$	0.718	94.192	3	8.1(−14)	25.01 ± 1.22	—	25.8	1.4(−15)
30	$^{240}\mathrm{Cm} \rightarrow {}^{32}\mathrm{Si} + {}^{208}\mathrm{Pb}$	0.733	97.825	0	3.7(−13)	21.48 ± 1.16	—	21.2	7.7(−16)

[a] Screening effect included (see equation (12)).

[b] $S = \exp(-G_{\mathsf{ov}})$; see equation (3).

[c] Taken from Ref. [16].

Figure Captions

Fig. 1 Shape of the one-dimensional potential barrier for ^{28}Mg decay of ^{234}U. The shaded area emphasizes the overlapping separation region a–c. In the external region c–b the barrier is described by the Coulomb potential (in cases of $\ell \neq 0$ the centrifugal barrier is also taken into account).

Fig. 2 Reduced radius, $R/A^{1/3}$, versus mass number, A, for emitted clusters (circles, equations (13) and (14)), and for daughter (triangles) and parent nuclei (squares) following the droplet model of atomic nuclei of [39, 40]. The line is the trend obtained along the beta-stability valley following the radius parametrization of [41] (see equations (13) and (14)).

Fig. 3 Finding the best g-value of the adjustable, one-parameter of the present model (equation (3)) through minimization of the standard deviation σ (equation (18)).

Fig. 4 Semiempirical g-values (points) for all cases of cluster emission experimentally investigated are shown in a); the dashed line indicates the average value, $\bar{g}$, and the shaded area the uncertainty (2σ). Part b) shows the difference $\Delta\tau = \log_{10}\left(T^{\mathsf{c}}_{1/2}/T^{\mathsf{e}}_{1/2}\right)$ between calculated and experimental half-life values, where the points can be seen distributed normally around $\Delta\tau = 0$ (see small histogram), and 80% of cases are of $|\Delta\tau| < 1$, i.e., most of the measured half-lives is reproduced by the present systematics within one order of magnitude. In part c) the calculated spectroscopic factor, $S = \mathrm{e}^{-G_{\mathsf{ov}}}$, is depicted for all cluster emission cases as indicated (the line is drawn to guide the eyes). The abscissa is the mass asymmetry parameter, η (equation (15)), and all data are those reported in table 1.

Fig. 5 Geiger-Nuttall-like plot for ^{14}C decay of $^{221\text{–}223}$Fr isotopes (circles), $^{221\text{–}226}$Ra isotopes (triangles), ^{223,225,227}Ac isotopes (squares), and ^{224,227}Th isotopes (reversed triangles). Full symbols are experimental data listed in table 1, and open ones represent calculated half-life values by the present model.

Fig. 6 Geiger-Nuttall-like plot for ^{16}O decay (circles), ^{18}O decay (triangles), and ^{20}O decay (squares) of thorium isotopes as indicated. Full symbol is the experimental datum for ^{228}Th$\rightarrow^{20}$O decay, and open symbols represent calculated half-life values by the present model.

Fig. 7 The same as in figure 5 for neon isotopes decay of uranium isotopes as indicated.

Fig. 8 The same as in figure 5 for ^{28}Mg decay of U, Np, and Pu isotopes, and ^{34}Si decay of Pu and Cm isotopes as indicated.

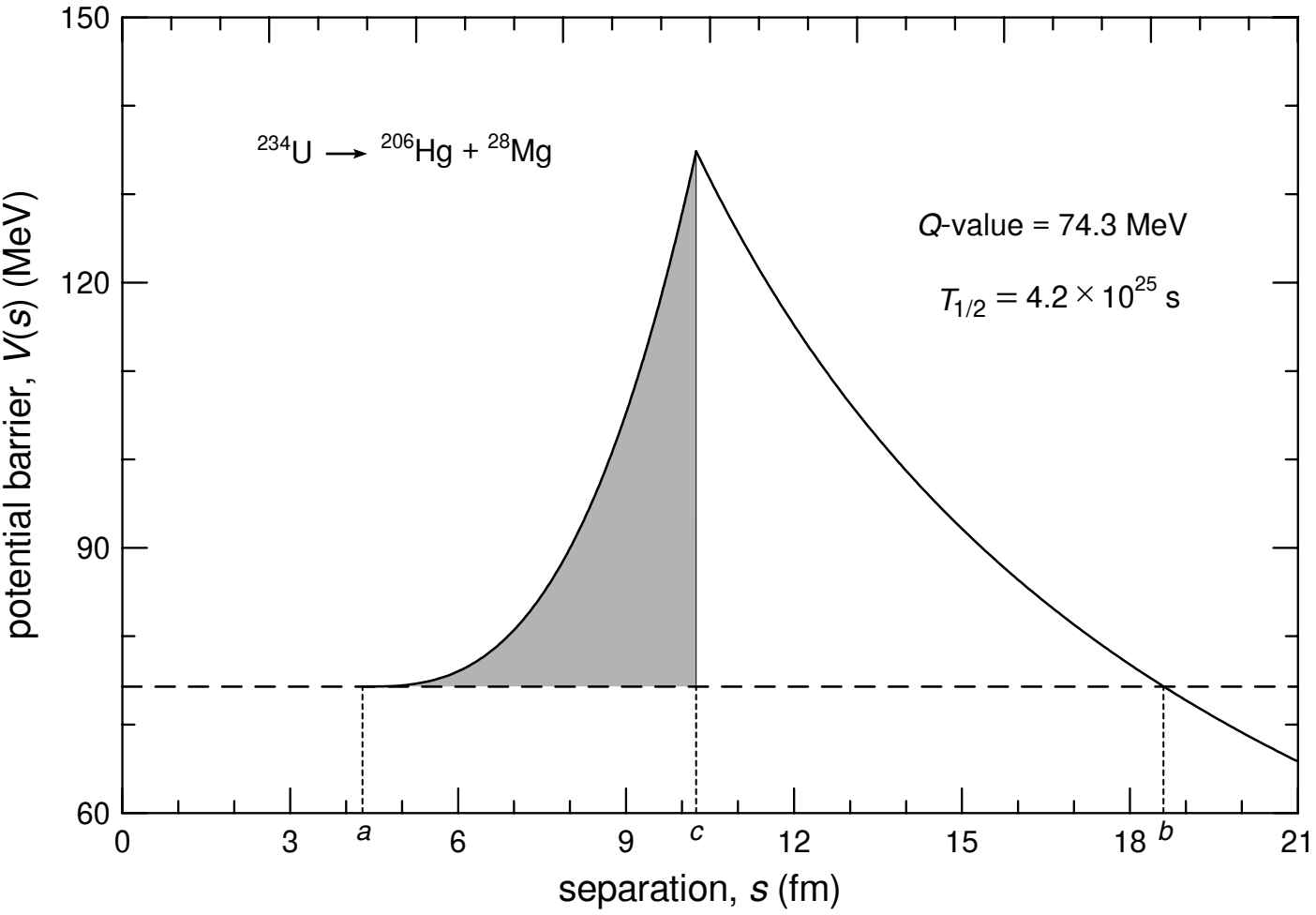
150
120
90
60
potential barrier, V(s) (MeV)
234U → 206Hg + 28Mg
Q-value = 74.3 MeV
T1/2 = 4.2 × 10^25 s
0
3
a
6
9
c
12
15
18
b
21
separation, s (fm)

Figure 1

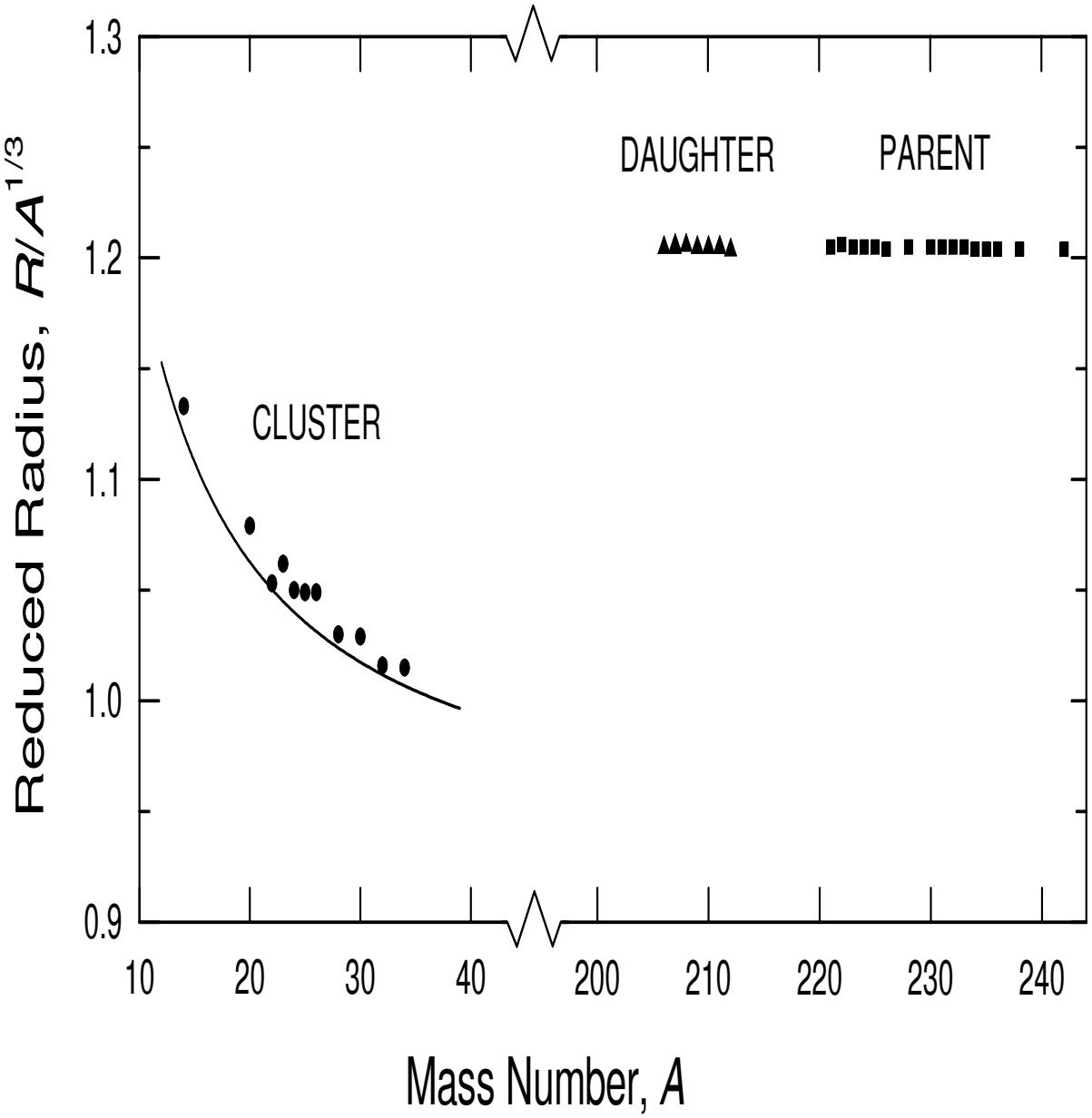
1.3
1.2
1.1
1.0
0.9
Reduced Radius, $R/A^{1/3}$
DAUGHTER
PARENT
CLUSTER
10
20
30
40
200
210
220
230
240
Mass Number, A

Figure 2

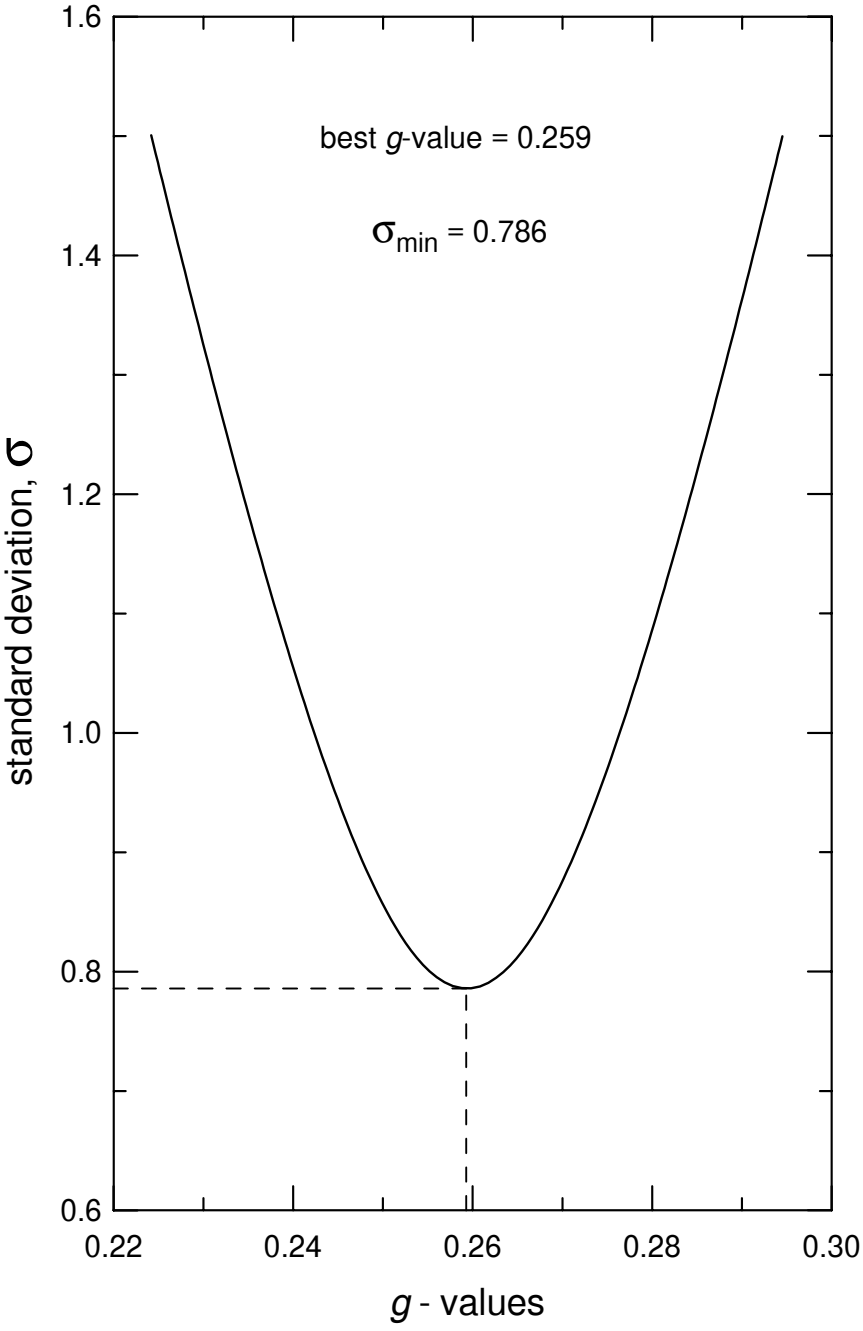
best g-value = 0.259
σmin = 0.786
standard deviation, σ
g - values
1.6
1.4
1.2
1.0
0.8
0.6
0.22
0.24
0.26
0.28
0.30

Figure 3

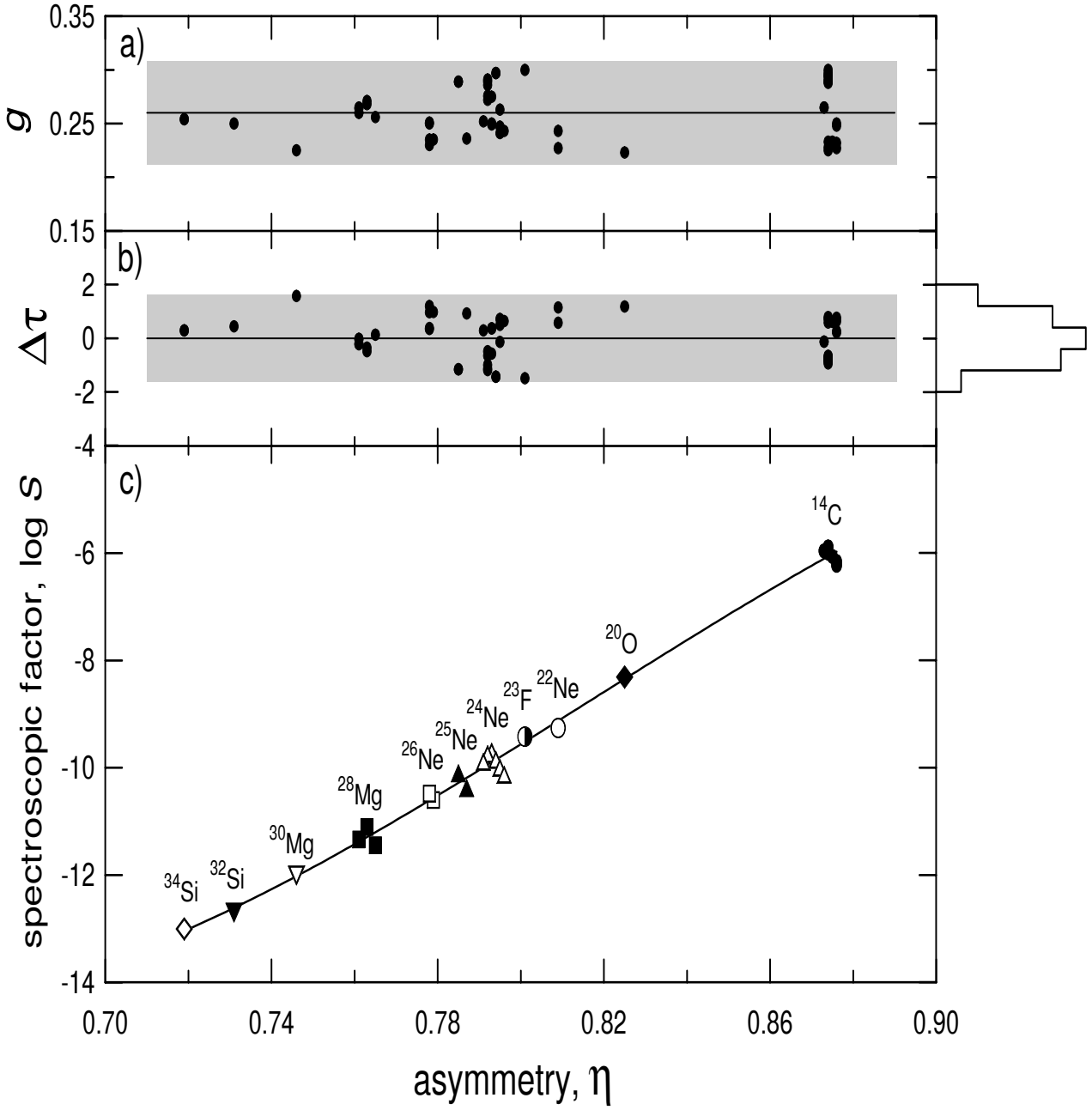
a)
b)
c)
g
Δτ
spectroscopic factor, log S
asymmetry, η
0.35
0.25
0.15
2
0
-2
-4
-6
-8
-10
-12
-14
0.70
0.74
0.78
0.82
0.86
0.90
14C
20O
22Ne
23F
24Ne
25Ne
26Ne
28Mg
30Mg
32Si
34Si

Figure 4

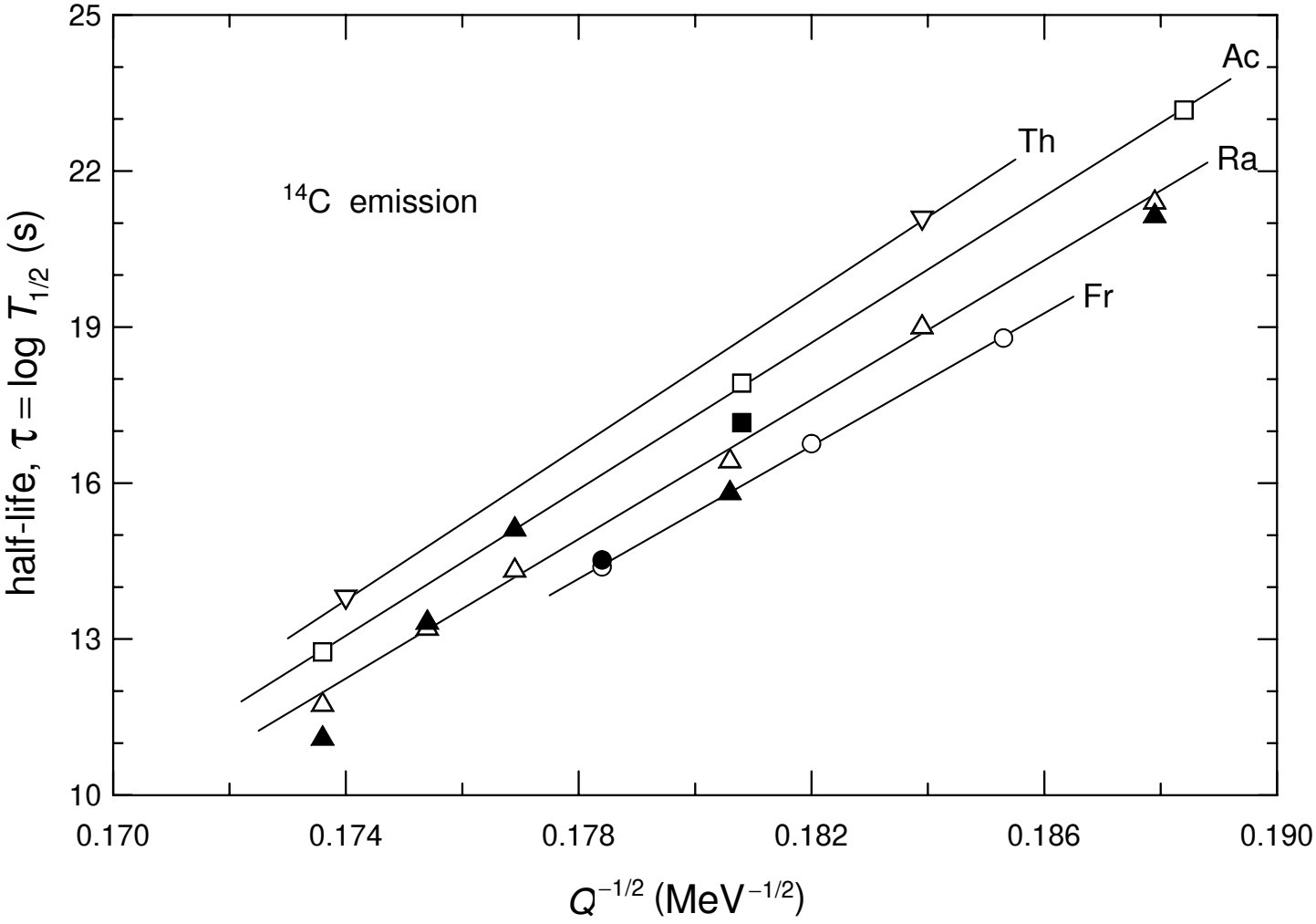
25
22
19
16
13
10
0.170
0.174
0.178
0.182
0.186
0.190
half-life, $\tau = \log T_{1/2}$ (s)
$Q^{-1/2}$ (MeV$^{-1/2}$)
^{14}C emission
Ac
Th
Ra
Fr

Figure 5

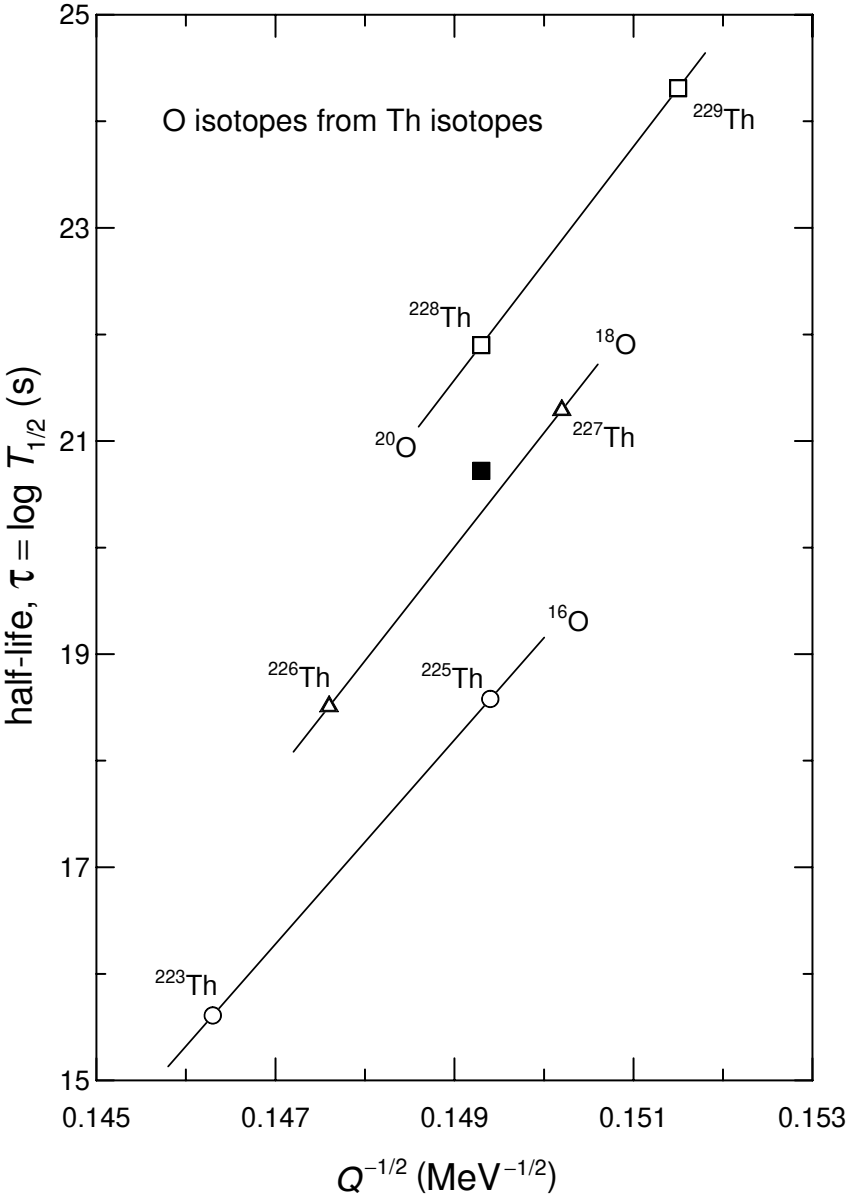
O isotopes from Th isotopes
229Th
228Th
18O
20O
227Th
16O
226Th
225Th
223Th
half-life, τ = log T1/2 (s)
Q−1/2 (MeV−1/2)
25
23
21
19
17
15
0.145
0.147
0.149
0.151
0.153

Figure 6

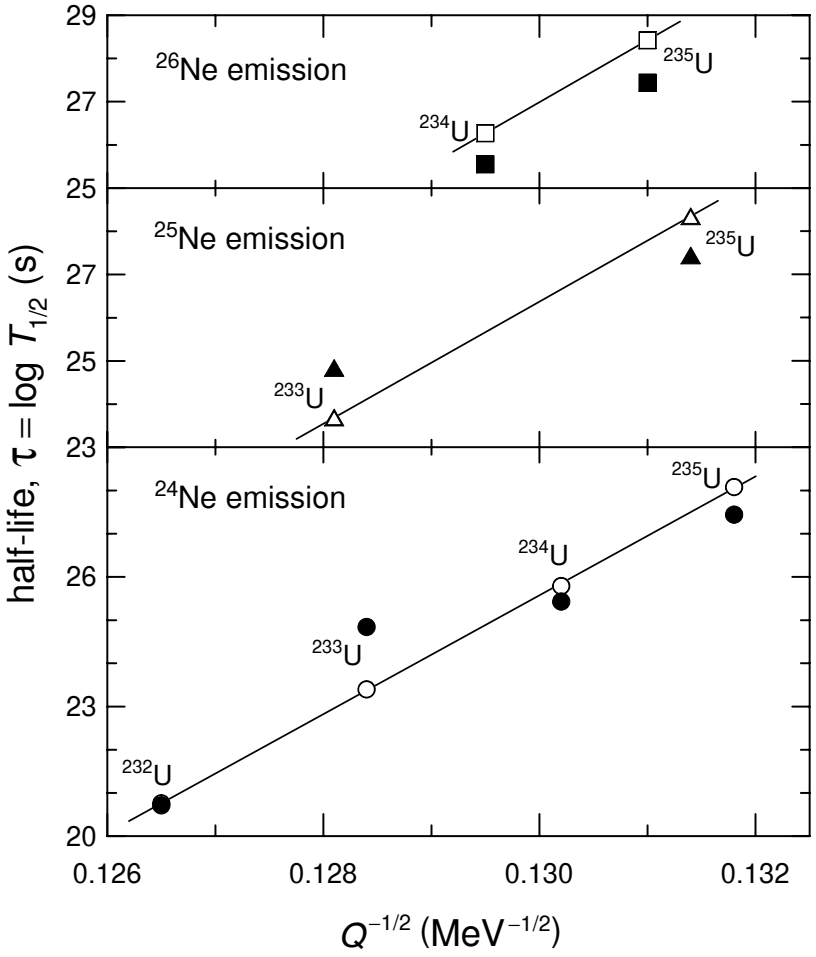
29
27
25
27
25
23
23
26
23
20
0.126
0.128
0.130
0.132
half-life, τ = log $T_{1/2}$ (s)
$Q^{-1/2}$ (MeV$^{-1/2}$)
^{26}Ne emission
^{25}Ne emission
^{24}Ne emission
^{234}U
^{235}U
^{233}U
^{235}U
^{235}U
^{234}U
^{233}U
^{232}U

Figure 7

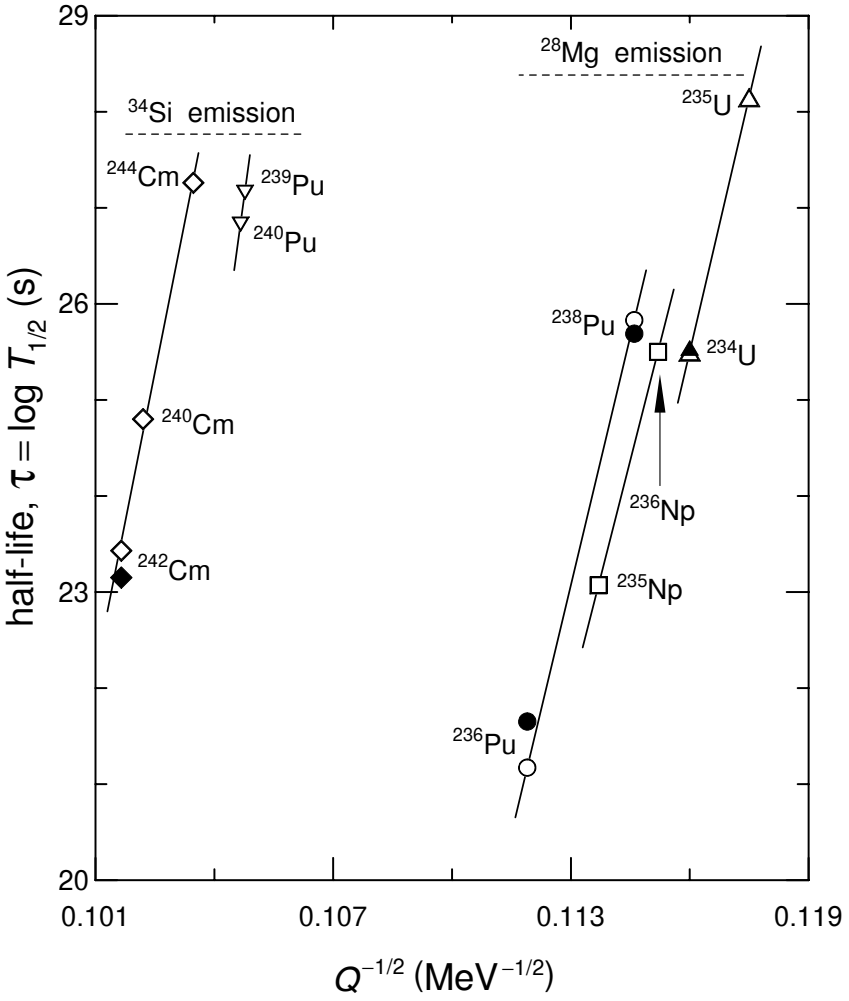
29
26
23
20
0.101
0.107
0.113
0.119
half-life, τ = log $T_{1/2}$ (s)
$Q^{-1/2}$ (MeV$^{-1/2}$)
^{34}Si emission
^{28}Mg emission
^{244}Cm
^{239}Pu
^{240}Pu
^{240}Cm
^{242}Cm
^{235}U
^{238}Pu
^{234}U
^{236}Np
^{235}Np
^{236}Pu

Figure 8